VOL. 13, NO. 6, MARCH 2018 ISSN 1819-6608
ARPN Journal of Engineering and Applied Sciences

www.arpnjournals.com

LINEAR AND NONLINEAR ACTIVE REJECTION CONTROLLERS FOR SINGLE-LINK FLEXIBLE JOINT ROBOT MANIPULATOR BASED ON PSO TUNER

Amjad J. Humaidi and Hussain M. Badir
Control and Systems Engineering Department, University of Technology, Baghdad, Iraq
E-Mai: 601116@uotechnology.edu.iq

ABSTRACT

This works presents two structures of active disturbance rejection controllers, Linear Active Disturbance Rejection Control (LADRC) and Nonlinear Active Disturbance Rejection Control (NADRC), to control single – link flexible joint robot manipulator. A comparison is made to evaluate the performance of suggested controllers in terms of transient characteristics. Moreover, the robustness capability of both controllers will be investigated with the presence of disturbance and uncertainty. One problem of NADRC and LADRC is they include various parameters which have an adverse effect on estimation process and, in turn, on the system performance unless they are properly tuned. Particle swarm technique (PSO) has been chosen as an optimal tuner to improve the estimation process and, thereby, to enhance the system performance.

Keywords: flexible joint robot, LADRC, NADRC, PSO.

INTRODUCTION

In flexible joint robot manipulators, the elasticity of the transmission devices on the joints has been taken into account. Considering the effect of joint flexibility would develop more exact model of industrial robot. However, a further complexity is added to robot model which raises a new control problem that motivated the researchers of relevant field to indulge in.

In the last three decades, many researchers have worked in the control of flexible joint robot. In [2], sliding mode control strategy has been applied to flexible joint manipulator. However, for feasible implementation of this control scheme, the design of controller requires the knowledge of uncertainty bounds and also the full information of all system states. In [3], a dynamic feedback control design is developed for the trajectory tracking control problem of robotic manipulators with flexible joints. In this control design, the position measurements of the link and motor are needed such hat a reduced-order observer is used to estimate the required velocities for controller. However, in this work, the establishment of system robustness requires certain conditions to be imposed on the uncertainties. In [4], the proposed controller is based on singular perturbation approach and the measurements of elastic force and position is a prerequisite for the control design. This work suggested nonlinear sliding state observer to estimate link velocities and elastic force time derivatives required for this control strategy. A controller design based on the integral manifold formulation [5], adaptive control [6], and a back-stepping approach [7] are some other approaches reported in the literature. It has been seen that majority of control designs in the literature require either information of full states or at least the position state or some state on motor side. Moreover, the guarantee of robustness may be highly dependent on systems model and demands the knowledge of some characteristics of uncertainties.

Active Disturbance Rejection Control (ADRC) was firstly proposed by J. Han with nonlinear gains. The control design of ADRC focused on nonlinear systems and considered both uncertain dynamics and disturbances. The essential idea of ADRC is firstly to lump both internal uncertain dynamics and external disturbances into a total uncertainty and then to estimate this lumped uncertainty by an extended state observer (ESO) and then to be cancelled out using state feedback structure. This makes ADRC applicable for many practical systems [1]. The nonlinear ADRC (NADRC) has been parameterized and modified to linear ADRC (LADRC) with linearized gains by Z. Gao [10]. ADRC requires little information of the plant and it is not completely dependent on the mathematical model of the system which makes it very robust against system uncertainty [1].

Recently, Active Disturbance Rejection Control (ADRC) has attracted the interest of many researchers in robotics. A method using ADRC has been proposed for control of a flexible joint robot in the control design used cascade nonlinear ADRC [9], and a feedback linearization (FL)-based control law based on ESO is presented in [8].

In the present work, two active disturbance rejection control schemes are presented, NADRC and LADRC, to control single-link flexible joint robot manipulator and the work contribution can be highlighted by the following points:

a) Performance comparison between linear and nonlinear ADRC is made in terms of dynamic behavior and robustness capability.

b) The suggested controllers have to control the nonlinear system structure of flexible joint manipulator without linearization.

c) A second order ADRCs have been used to control fourth order system.

d) PSO technique is included to improve the closed-loop system performance.

JOINT FLEXIBILITY AND SYSTEM MOD-ELING

The Modelling, simulation and real-time control of flexible manipulators is still challenging and an open problem. Many academic and industrial researches have considered flexibility at joints due to its significant effect and it may dominate over link flexibility at the majority of the manipulators available nowadays. This can be seen in many applications where industrial robotic manipulators are driven by harmonic drive gears [11].

The flexibility at a joint cab modelled by a linear, torsional spring as indicated figure (1). It is clear that motor drive the arm via a spring attached to motor shaft [12].

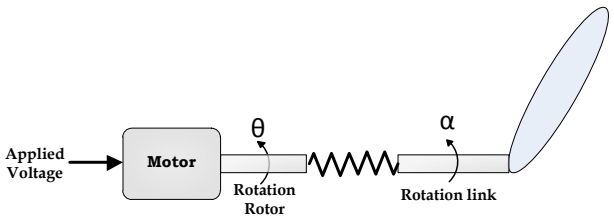

Figure-1. Flexible joint robot.

The modeling of a single–link flexible joint robot is considered operating on a vertical plane and developed using Lagrange method. The method is based on conservation of energy and it is initiated by finding the difference between kinetic energy K and the potential energy P of all system components [12]

$$L = K - P \tag{1}$$

Then, Lagrange equations are configured as follows:

$$\frac{d}{dt}\frac{dL}{d\dot{\alpha}} - \frac{dL}{d\alpha} = 0 \tag{2}$$

$$\frac{d}{dt}\frac{dL}{d\dot{\theta}} - \frac{dL}{d\theta} = \tau \tag{3}$$

Based on Figure-1, the following equations can be derived [12],

$$J_l\ddot{\theta} + J_l\ddot{\alpha} + K_s\alpha - mgh\sin(\theta + \alpha) = 0 \tag{4}$$

$$(J_h + J_l)\ddot{\theta} + J_l\ddot{\alpha} - mgh\sin(\theta + \alpha) = \tau \tag{5}$$

Using Kirchhoff's voltage law (KVL) and neglecting the motor inductance, the electrical side of the system gives

$$v = iR_m + K_mK_g\omega$$
$$i = (v/R_m) - (K_mK_g\omega/R_m) \tag{6}$$

where ω is the angular velocity of the motor ($\dot{\theta} = \omega$), v is the applied input voltage, R_m is the armature resistance, K_m motor gain and K_g is the gear ratio. The current is related to developed torque τ by the following equation,

$$\tau = K_mK_g i \tag{7}$$

Then, one can deduce from Equation. (7) and (6) that

$$\tau = K_mK_g\,(v/R_m) - (K_m^2K_g^2\,\omega/R_m) \tag{8}$$

Substituting Equation. (4) into Equation. (5) yields

$$J_h\ddot{\theta} - K_s\alpha = K_mK_g\,v/R_m + K_m^2K_g^2\,\omega/R_m$$

or,

$$\ddot{\theta} = \left(K_mK_g/J_hR_m\right)v - (K_m^2K_g^2/J_hR_m)\,\dot{\theta} + \left(\frac{K_s}{J_h}\right)\alpha \tag{9}$$

From Equation. (9) and Equation. (4), one can get

$$\ddot{\alpha} = -\left(K_mK_g/J_hR_m\right)v + (K_m^2K_g^2/J_hR_m)\,\dot{\theta} - (K_s/J_h)\,\alpha - (K_s/J_l)\,\alpha + (mgh/J_l)\,sin(\theta + \alpha) \tag{10}$$

The arm angle (tip angle) is composed of the sum α and θ. Letting $x_1 = \theta$, $x_2 = \alpha$, $x_3 = \dot{x}_1 = \dot{\theta}$, $x_4 = \dot{x}_2 = \dot{\alpha}$, then the system described by Equation. (9) and Equation. (10) can be written in state variable form [14]:

$$\dot{x_1} = x_3$$
$$\dot{x_2} = x_3$$
$$\dot{x_3} = \left(K_mK_g/J_hR_m\right)v - (K_m^2K_g^2/J_hR_m)\,x_3 + (K_s/J_h)\,x_2$$
$$\dot{x_4} = -\left(K_mK_g/J_hR_m\right)v + (K_m^2K_g^2/J_hR_m)\,x_3 - (K_s/J_h)\,x_2 - (K_s/J_l)\,x_2 + (mgh/J_l)\sin(x_1 + x_2)$$
$$y = x_1 + x_2 \tag{11}$$

Active disturbance rejection control

Structure of the nonlinear ADRC

The nonlinear ADRC controller consists of two main parts; tracking differentiator (TD) and Nonlinear Extended State Observer (NESO). The task of tracking differentiator is to manage the transient process and, in addition, if the input is corrupted by noise, then appropriate filters and tracking differentiator are used to remove noise effect. The mathematical description of TD is generally given by [14],

$$\dot{z}_1 = z_2$$
$$\dot{z}_2 = f_h$$
$$f_h = f_{han}(z_1 - v, z_2, r, h) \tag{12}$$

where v is the input signal, r is called the speed factor, h is the filter factor and $f_{han}(x_1, x_2, r, h)$ is the integrated function of time optimum control, which is given by;

$$f_{han} = \begin{cases} r.sign(a) & |y| > d \\ r\dfrac{a}{d} & |y| \le d \end{cases} \tag{13}$$

where,

$$a = \begin{cases} x_1 + \dfrac{(ao - d)}{2} sign(y), & |y| > do \\ x_2 + \dfrac{y}{h}, & |y| \le do \end{cases} \quad (14)$$

$$d = r.h$$
$$d_o = h.d$$
$$y = x_1 + x_2 .h$$
$$a_o = \sqrt{d^2 + 8.r.|y|}$$

For the position control of single–link flexible joint robot manipulator, the angle of flexible joint robot, z_1, track the angle of flexible joint robot, z_2, track the differential signal.

The second element of Nonlinear ADRC is Nonlinear Extended State Observer (NESO). This structure of observer was proposed by J. Han in 1995 and characterized by independency of plant mathematical model and thus achieving inherent robustness. The descriptive model is given by

$$\begin{aligned} e &= z_1 - y \\ \dot{z}_1 &= z_2 - L_1.e \\ \dot{z}_2 &= z_3 - L_2.fal(e, \alpha_1, \delta_1) + b.u \\ \dot{z}_3 &= -L_3.fal(e, \alpha_2, \delta_2) \end{aligned} \quad (15)$$

where e is the error between actual and estimate output of system,L_1,L_2, L_3 represent the gains of observer,z_1 , z_2 are the estimates of the states x_1 and x_2. The state variable z_3 is the estimate state of lumped uncertain, nonlinearity and disturbances (external and internal) of the system. The function $fal(e, \alpha, \delta)$ is a nonlinear function

$$fal(e, \alpha, \delta) = \begin{cases} \dfrac{e}{\delta^{\alpha-1}}, & |e| \le \delta \\ |e|^{\alpha} sign(e), & |e| > \delta \end{cases}$$

which yields high gain when error is small, α is chosen between (0 and 1), δ is a small number used to limit the gain in the neighbourhood of origin.

The third part of NADRC is the nonlinear state error feedback (NLSEF). The mathematical structure of NLSEF is given by

$$\begin{aligned} e_1 &= v_1 - z_1 \\ e_2 &= v_2 - z_2 \\ u_o &= k_p.fal(e_1, \alpha_1, \delta_1) + k_d.fal(e_2, \alpha_2, \delta_2) \\ u &= u_o - \frac{z_3}{b} \end{aligned} \quad (16)$$

where e_1, e_2 represent the error between input signals and the estimate states of system, k_p, k_d are gains of NLSEF, $fal(e_1, \alpha_1, \delta_1)$, $fal(e_2, \alpha_2, \delta_2)$ are the nonlinear functions of NLSEF.

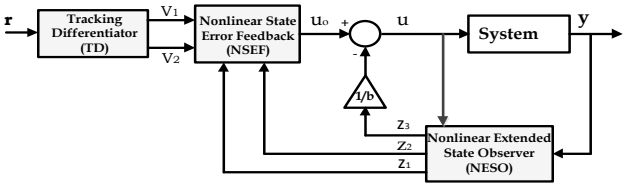

Figure-2. A schematic representation of NADRC.

Structure of the linear ADRC

The structure of LADRC controller is composed of ESO (Extended State Observer) and SEF (State Error Feedback). The tracking differentiator has been omitted in the present structure and, due to simplicity in parameter tuning, the linear extended state observer (LESO) has been used, which a linear version of nonlinear extended state observer (NESO). The mathematical structure of LESO can be described by the following

$$\begin{aligned} e &= y - z_1 \\ \dot{z}_1 &= z_2 + L_1.e \\ \dot{z}_2 &= z_3 + L_2.e + b.u \end{aligned} \quad (17)$$

$$\dot{z}_3 = L_3.e$$

where L_1, L_2 and L_3 are the observer gains and the variable z_3 stands for lumped disturbance, uncertainty together with system nonlinearity. The second element of LARC is LSEF which can be represented by the following set of equations

$$\begin{aligned} e_1 &= v_1 - z_1 \\ e_2 &= v_2 - z_2 \\ u_o &= k_p.e_1 + k_d.e_2 \end{aligned} \quad (18)$$

$$u = u_o - z_3/b$$

where e_1, e_2 represent the error between input signals and estimate states of system, k_p, k_d are the gains of linear state feedback (LSEF). Figure (4) shows the schematic diagram of linear ADRC.

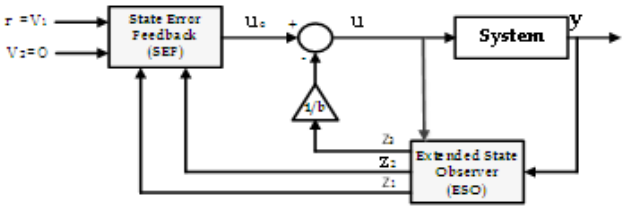

Figure-3. A schematic representation of LADRC.

ACTIVE DISTURBANCEREJECTION CONTROL-BASEDON PSO

The original ADRC system has many parameters, which are required to be tuned to improve the controller capabilities. Due to complexity of ADRC and tight coupling of its constituting parameters, try and error tuning process is exhaustive and does not lead to global optimizing solutions and, as such, an alternative optimization technique is required. In the present work, particle swarm optimization (PSO) technique has been

chosen for tuning purposes. PSO algorithm is based on the behavior of individuals of swarm. These individuals share information among them and this leads to increased efficiency of the group [13]. This optimization method will not only responsible for tuning of all parameters, but also to find the best value for it, which achieve minimum error between desired and actual states or between the inputs and outputs of the system.

Using PSO technique rather than try-and-error procedure will improve the estimation process and hence the closed-loop system dynamic is better enhanced due to improved estimates of observer. It is evident that the number of parameters associated with LADRC is much less than that for NADRC. The numeric values given in the above tables represent the optimal values of parameters which are tuned based on estimation error minimization. The fitness function composed by RMSE (root mean square error) index is adopted in comprehensive consideration of the rapidity, stability and accuracy of system.

$$J(RMSE) = \sqrt{\frac{\sum_{i=1}^{n} e^2}{n}}$$

Parameterization method is proposed by Gao [10] to tune parameter of LADRC. The parameterization method find the gains value of both controller and observer based on bandwidth of observer ω_0 and controller ω_c. This can be clarified using the relationship between controller gains and its bandwidth frequency ω_c;

$$\lambda(s) = s^2 + k_d s + k_p = (s + \omega_c)^2$$

where $k_d = 2\omega_c,\ k_p = {\omega_c}^2$. Similarly, based on the following equation, which relates observer gains and its bandwidth, the observer gains can be obtained

$$\lambda(s) = s^3 + L_1 s^2 + L_2 s + L_3 = (s + \omega_0)^3$$

where $L_1 = 3\,\omega_0,\ L_2 = 3\,\omega_0^2,\ \ L_3 = \omega_0^3$. Thus, this method could simplify the level of complexity to find the optimal gain values of LESO and NESO based on PSO. Table-1 list the optimal parameters of NESO, NLSEF and TD, which have been tuned by PSO algorithm. On the other hand Table-1 gives the optimal parameters of LESO and LSEF resulting from PS optimizer.

Table-1. Optimal parameters of NADRC.

NESO. Param.	Value	NLSEF. Param.	Value	TD. Param.	Value
ω_o	17.979	ω_c	1.7979	r	8
L_1	53.9	β_1	3.2324	h	0.000001
L_2	969.7	β_2	3.5958		
L_3	5811.6	α_1	0.9		
b	46.3634	δ_1	0.00001		
α_1	1	α_2	1.25		
δ_1	0.1	δ_2	0.00001		
α_2	0.98				
δ_2	0.1				
α_3	0.78				
δ_3	0.1				

Table-2. Optimal parameters of LADRC.

LESO. Param.	Value	LSEF. Param.	Value
ω_o	17.979	ω_c	1.7979
L_1	53.9	β_1	3.2324
L_2	969.7	β_2	3.5958
L_3	5811.6		
b	46.3634		

THE NUMERICAL SIMULATION AND RESULTS

In this section, the dynamic behavior of flexible-joint system, based on ADRC, is established using MATLAB/Simulink. The numeric values of system parameters are listed in Table-3. The first comparison is made based on how well the transient characteristics could be given by such controllers. The controller reference input is assigned to be step input of height 30^0 and the tip angle $(\theta + \alpha)$ is the output response, which has to be controlled. Figure-5 shows the dynamic behaviors of flexible-joint system resulting from both controllers. The figure shows that NADRC give better transient characteristics than LADRC. Table-4 makes a quantitative comparison based on simulation, which confirms that response due to NLADRC outperforms the response resulting from LADRC. The key index of comparison is measured by root means square error (RMSE) which

calculate the root mean square of error over the entire response. The response with less RMSE will address the best controller.

Table-3. Numerical values of system parameters [12].

Parameter	Symbol	Value
Load Inertia	J_l	0.0059 [$kg.m^2$]
Inertia of hub	J_h	0.0021 [$kg.m^2$]
Link Mass	m	0.403 [kg]
Height of C.M.	h	0.06 [m]
Spring Stiffness	K_s	1.61 [N/m]
Motor Const.	K_m	0.00767
Gear Ratio	K_g	70
Motor Resist.	R_m	2.6 [Ω]
Gravity Const.	g	-9.81 [N/m]

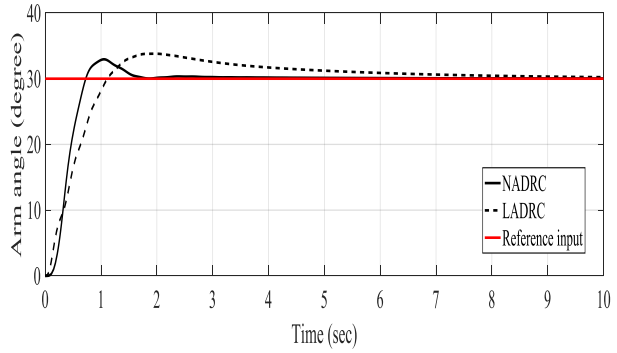

(a) Tip angle

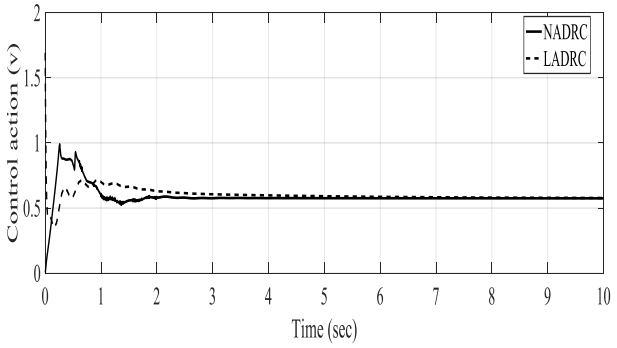

(b) Control signal

Figure-4. Performance of NADRC and LADRC with nominal case.

Table-4. Dynamic performance report of controllers.

Controller	RMSE	Max overshoot%	Settling time(sec.)
LADRC	9.7576	3.8	7.133
NADRC	2.9558	2.93	1.54

Another comparison is made to assess the robustness capabilities of suggested controllers due to changes of system parameters. Two parameters are varied in discrete form from their nominal values; link mass and link length. It is worthy to notify that the change of such parameters is considered to impose hypothetical parameter variation and and there is not the case in practical situation. Figure-5 and Figure-6 show the dynamic responses of tip angle and control signals resulting from LADRC and NLADRC, respectively. The responses indicated in the figures correspond to three values of masses (nominal value of mass, two times nominal value of mass, three times nominal value of mass). Similarly, Figure-8 and Figure-9 shows the transient responses of tip angle and control signals due to LADRC and NLADRC, respectively. The three behaviors shown in the figures stand for different link lengths; nominal length, 25% of nominal length and 50% of nominal length. Table-5 gives a summary of robustness capability for both controllers and reports the deviation from the nominal, measured in RMSE, for both controllers when the system is subjected to parameter variations. It is evident from the table that the minimum deviation from the nominal occurs with LADRC and this indicates that this controller outperforms NLADRC in terms of robustness characteristics

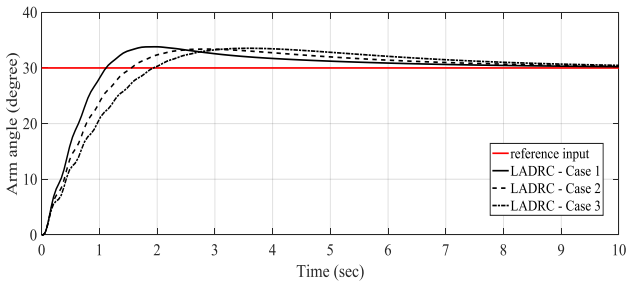

(a) Tip angle

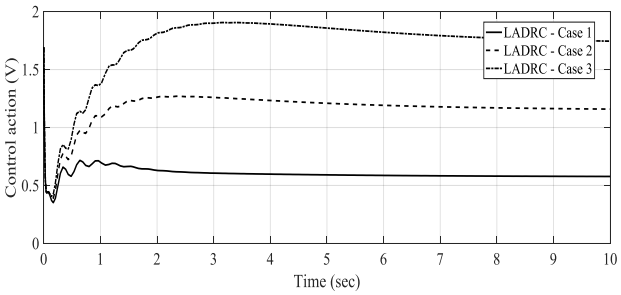

(b) Control signal

Figure-5. Dynamic responses of LADRC with three different setting of mass.

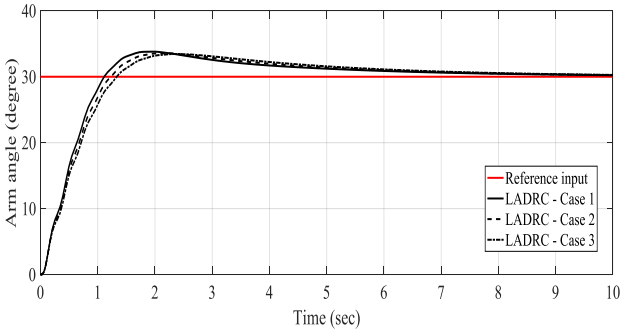

(a) Tip angle

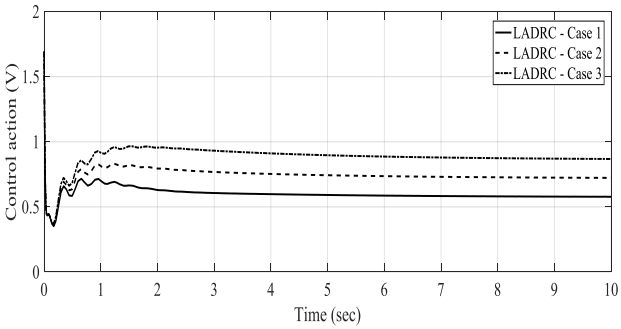

(b) Control signal

Figure-6. Dynamic responses of LADRC with three different setting of link length.

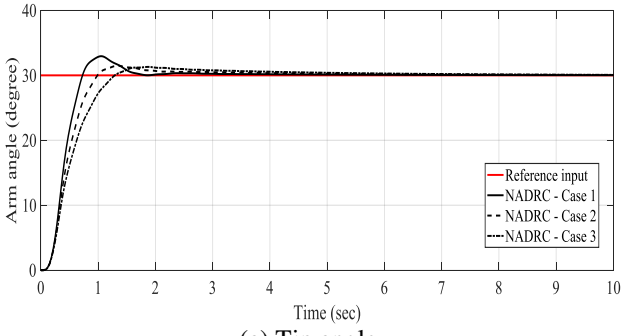

(a) Tip angle

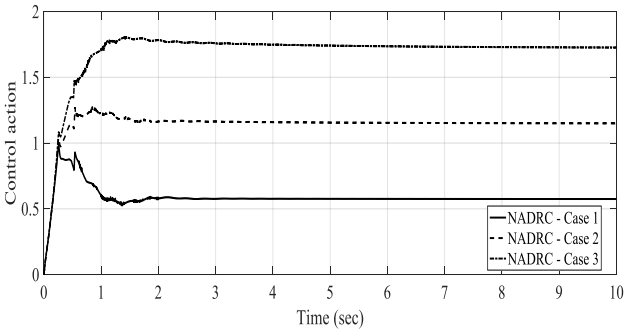

(b) Control signal

Figure-7. Dynamic responses of NADRC with three different setting of mass.

Table-5. Robustness evaluation of controllers.

Percentage change of parameters	RMS of LADRC	Percentage change (LADRC)	RMS of NADRC	Percentage change (NLADRC)
+100% of mass	10.0449	2.9444%	3.2800	10.9683 %
+200% of mass	10.4050	6.6348%	3.9296	32.9454 %
+25% of length	9.8043	0.4786%	3.0286	2.4630 %
+50% of length	9.8813	1.2677%	3.2540	10.0886 %

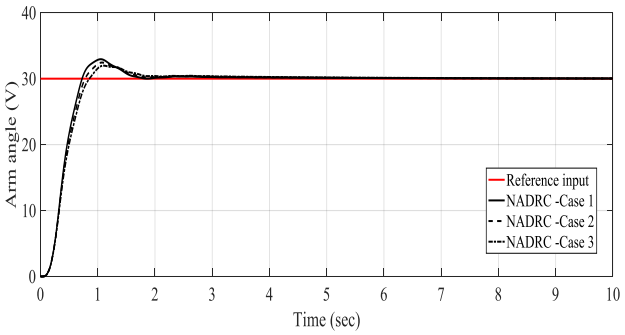

(a) Tip angle

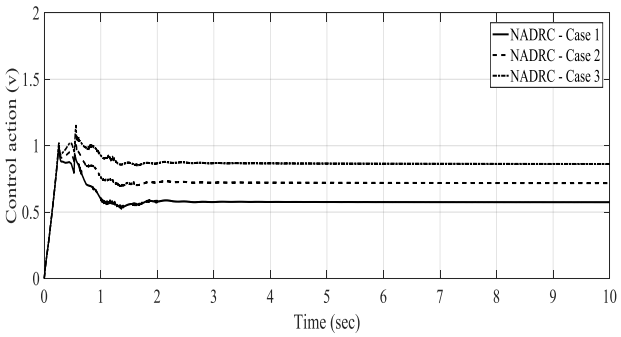

(b) Control signal

Figure-8. Dynamic responses NADRC with three different setting of link length.

CONCLUSIONS

This paper presents a comparison study between two active rejection disturbance controllers in terms of transient characteristics and robustness. Based on simulated results, one can conclude that NLADRC give better dynamic behavior than LADRC. However, LADRC has better robustness capabilities than NLADRC when the system is subjected to a variation of parameters. PSO has played a vital role in optimization and performance enhancement of overall active rejection disturbance-controlled system.

REFERENCES

[1] J. Han. 2009. From PID to Active Disturbance Rejection Control. IEEE Transactions on Industrial Electronics. 56(3): 900-906.

[2] S. K. Spurgeon, L. Yao and X. Y. Lu. 2001. Robust tracking via sliding mode control for elastic joint manipulators. Proc. Inst. Mech. Eng. I, 215(4): 405-417.

[3] Y. C. Chang, B. S. Chen and T. C. Lee. 1996. Tracking control of flexible joint manipulators using only position measurements. Int. J. Control. 64(4): 567-593.

[4] J. Hernandez and J.-P. Barbot. 1996. Sliding observer-based feedback control for flexible joints manipulator. Automatica. 32(9): 1243-1254.

[5] M. W. Spong. 1987. Modeling and control of elastic joint robots. Trans. ASME, J. Dyn. Syst., Meas., Control. 109(4): 310-319.

[6] F. Ghorbel, J. Y. Hung and M. W. Spong. 1989. Adaptive control of flexible joint manipulators. IEEE Control Syst. Mag. 9(7): 9-13.

[7] J. Oh and J. Lee. 1999. Control of Flexible Joint Robot System by Backstepping Design Approach. Intelligent Automation & Soft Computing. 5(4): 267-278.

[8] S. Talole, J. Kolhe and S. Phadke. 2010. Extended-State-Observer-Based Control of Flexible-Joint System with Experimental Validation. IEEE Transactions on Industrial Electronics. 57(4): 1411-1419.

[9] Y. Zhao, Z. Zhao, B. Zhao and W. Li. 2011. Active Disturbance Rejection Control for Manipulator Flexible Joint with Dynamic Friction and Uncertainties Compensation. Fourth International Symposium on Computational Intelligence and Design. 2(1): 248-251.

[10] Z. Gao. 2003. Scaling and bandwidth-parameterization based controller tuning. Proceedings of the 2003 American Control Conference, 2003. 6(7): 4989-4996.

[11] B. Siciliano and O. Khatib. 2008. Springer handbook of robotics. Berlin: Springer. pp. 287-295.

[12] A. Dehghani and H. Khodadadi. 2016. Self-Tuning PID Controller Design Using Fuzzy Logic for Single-Link Flexible Joint Robot Manipulator. Journal Teknologi. 78(6-13).

[13] Z. Gaing. 2004. A Particle Swarm Optimization Approach for Optimum Design of PID Controller in AVR System. IEEE Transactions on Energy Conversion. 19(2): 384-391.

[14] F. Meng, J. Yang, P. Yang and B. Sun. 2012. The Research of Frequency Characteristics of Tracking Differentiator. Applied Mechanics and Materials. 182-183: 1474-1478.